Determining Camera Spectral Responsivity with Multispectral Transmission Filters

Lindsay W. MacDonald; 3DIMPact Research Group, Faculty of Engineering, University College London; UK

Abstract

Four practical methods were evaluated for determining the spectral responsivity of a Nikon D200 digital camera: (1) Direct measurement by exposure to a monochromator sequence at 5nm intervals; (2) LED colour target with 36 luminous circular patches; (3) filtered illumination, using 16 transmission filters of 20nm bandwidth; (4) filtered camera, using the same set of filters. Taking the monochromator measurements as the reference, the results of the other three methods showed a good correspondence, but systematic differences were observed for fluorescent illumination. Because of the wavelength shift in filter transmittance with angle of incidence, it is recommended that sources with smooth spectral power distributions should be used for filter-based characterisation.

1. Introduction

Colorimetric calculations for digital photography require a knowledge of the spectral responsivity of each colour channel of the camera. Numerous studies have shown how this can be measured directly by using a narrowband (near monochromatic) light source, presented to the camera via one port of an integrating sphere or by reflection from a matte white tile. The wavelength of the source is scanned through the full visible spectrum, and the camera's RGB output signals recorded at each wavelength. The three sensitivity curves are then obtained by interpolating the measured values by cubic splines to obtain a continuous curve. Vora *et al* measured the responses of two Kodak digital cameras [1]. Martínez-Verdú *et al* measured the spectral responsivity of a Sony DXC-930P digital camera [2]. Wu and Allebach used a monochromator and tungsten-halogen light source to generate 31 colour stimuli of 10 nm bandwidth to measure the sensitivity of a Kodak DCS460c camera [3]. MacDonald and Ji characterised a medium-format Rollei with a Jenoptik digital back by measurements from a monochromator at 5 nm wavelength intervals, and showed that the performance of the spectral measurement method was good enough to yield low mean-square errors when predicting the colours of a calibration target [4].

Instead of the monochromator, which is expensive and difficult to set up, an easier alternative method is to use a set of narrow-band transmission filters at intervals across the visible spectrum. The camera integrates the response over the waveband transmitted by each filter and thus the sensitivity of each channel is sampled at regular intervals [5]. With the aid of a spectroradiometer, the method facilitates camera characterisation as the basis of comparison for the accuracy of spectral estimation techniques [6].

The camera used in this study was a Nikon D200, in which the sensitivity of each R,G,B channel is a product of transmittance of the Bayer mask filters, infra-red cutoff filter and the sensitivity of the CCD silicon sensor [7]. The photosites are 6.05 µm square, and the DX-format image size is 3900x2600 pixels (nominally 10.1 Mpixels in 3:2 aspect ratio). Because Nikon provides no data on colour sensitivity, it was necessary to characterise the responsivity of the three channels as a function of wavelength. Four different methods were compared, all working from basic physical principles.

2. Monochromator

The responses of the three channels of the Nikon D200 camera were measured directly by exposure to the light output from a monochromator. The Bentham FSGM-150 instrument passed white light from a pulsed xenon source through a diffraction grating to produce light of 10 nm bandwidth (at half maximum amplitude), variable at 5nm intervals over a wavelength range from 380 to 780 nm. The light was transmitted through an optical fibre bundle to one port of an integrating sphere, and was imaged through the second port (Fig. 1). The wavelength of the output light was controlled by the voltage from an external stabilised power supply, calibrated by a set of measurements by a Minolta CS-1000 spectroradiometer.

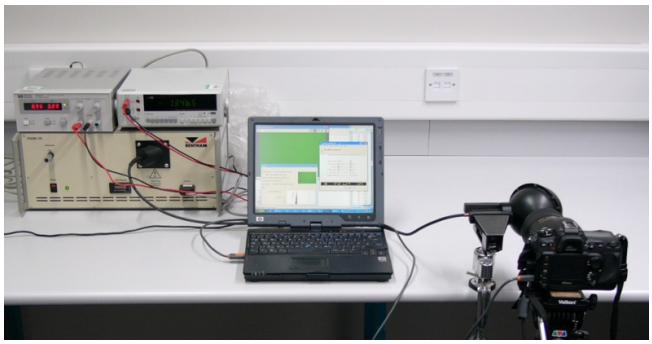

Figure 1. Setup on laboratory bench for measurement of spectral response of the Nikon D200 camera.

All images were captured in a darkened room. For each wavelength setting an image of the light seen through the port of the integrating sphere was taken by the camera, with a shutter speed of 4 seconds, sensitivity of ISO100 and lens aperture f/5. The images were linearised via the DCRAW software utility and a region of 200x200 pixels cropped from each image within the area of the sphere port. The 16-bit pixel values in the cropped area of each image were averaged to give the 'raw' camera response of each channel as a function of wavelength.

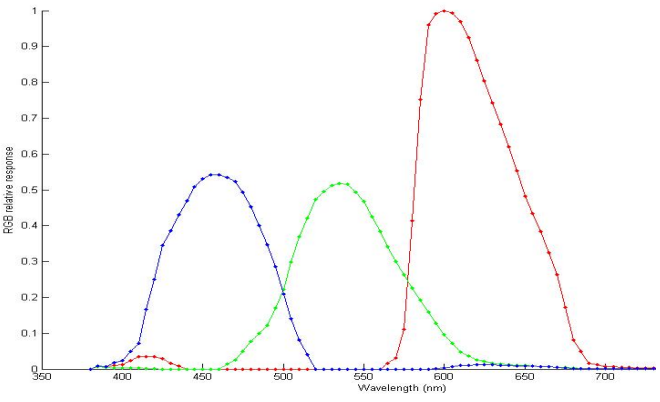

Figure 2. Normalised sensitivity vs wavelength at 5nm intervals for the red, green and blue channels of the Nikon D200 camera.

The mean pixel intensity values were corrected by dividing at each wavelength by the integrated power of the lamp, and interpolated by cubic splines, yielding sensitivity curves for the three channels (Fig. 2). The curves are broad and overlapping, giving good coverage of all regions of the visible spectrum, with an average bandwidth of approximately 80nm. It is unclear why the peak sensitivity of the red channel is nearly double that of green and blue, but probably the result of greater sensitivity of the silicon sensor at longer wavelengths. Because of the RAW image capture method, no white balance scaling had been performed by the camera on the signal values. See Section 6 for discussion of white balance.

3. LED Spectral Target

A custom LED colour target [8] was tested as a quick means of characterisation of the camera's spectral sensitivity (Fig. 3). It consisted of 36 luminous circular patches in a box with an active area of c.10x10 cm. Each patch had a narrow-band interference filter of approximate bandwidth 10nm in front of an LED source, and the overall ensemble sampled the spectrum from 380 to 730 nm at 10nm intervals. It therefore enabled the spectral sensitivity of each channel to be determined in a similar manner to the use of a variable monochromatic source, but with a single exposure by the camera. DiCarlo *et al* previously demonstrated a similar device [9].

Figure 3. Laboratory setup for spectral measurement by PR-650 (foreground)

The power of each patch of the target was measured with a PhotoResearch PR-650 spectroradiometer, giving the radiance at 4nm intervals over the range 380-780 nm, a vector of 101 values per patch. The target was captured as an image by the Nikon D200 at ¼ sec with the 105 mm lens set to aperture f/8, at a distance of approximately 80 cm. The image was saved in raw format (NEF file) and converted via DCRAW to 16-bit linear TIFF. The mean values of the R,G,B channels were determined from an area of 101x101 pixels at the centre of each patch in the image. Correction factors could have been derived from the maximum power of each lamp, assuming that they were evenly spaced at 10 nm intervals. Improved factors were determined from the measured power for each patch in the target as follows: the 'true' wavelength was calculated as the centroid of the curve, using a weighted summation over all wavelengths, with the amplitude as a linear weighting coefficient; then the total (integral) power was calculated as the area under the curve, by summation over all wavelengths. Dividing the pixel intensity values by the corresponding radiant power values for each patch and plotting against the centroid wavelength gave the spectral sensitivity of each channel (Fig. 4). The three curves were normalised to set the maximum value (red channel) to 1.0.

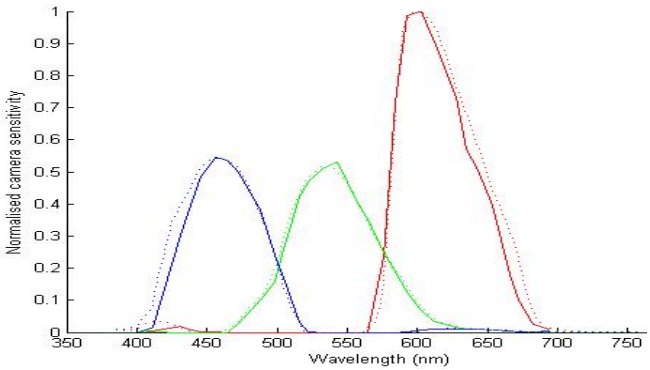

Figure 4. Corrected sensitivity of R,G,B channels for LED target (solid lines) vs sensitivity from variable monochromator (dotted lines).

The results showed good agreement with the characterisation by the variable monochromator, except for a sliver of difference on the short-wavelength side of blue and the long-wavelength side of red. These differences could perhaps be explained by a lower response from the camera than expected for the blue patches in the upper rows of the chart and the red patches in the lower rows of the chart, because of vignetting of intensity by the lens and/or angular attenuation of the light transmitted through the interference filters. Both effects could be mitigated by imaging the target from a greater distance so that it subtended a smaller angle of view to the camera.

4. Multispectral Filters on Illumination

A set of 16 glass dichroic transmission filters from a multispectral image capture system was used, with central wavelengths at intervals of 20nm throughout the visible spectrum from 400 to 700 nm inclusive, each with a bandwidth of approximately 20nm. These filters had previously been used for multispectral image capture of damaged parchment [10].

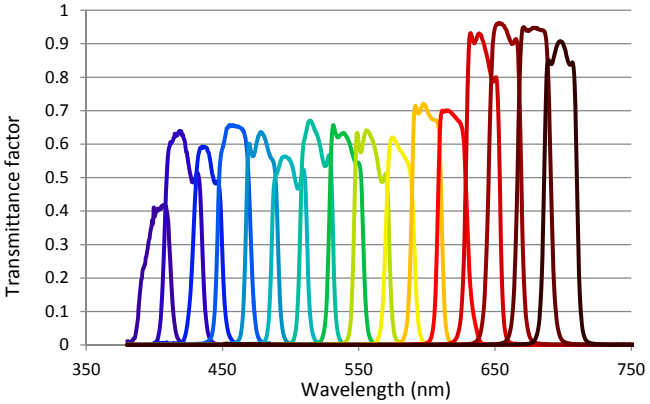

Figure 5: Measured transmittance factors for 16 filters.

Each filter was a glass disc 50mm in diameter and was mounted in an assembly of lens adapter rings, so that it could be screwed directly into a standard 52mm threaded mount. The spectral transmittance of each filter was measured directly with an Ocean Optics HR2000+ spectrometer. Light from a tungsten halogen source was passed through a diffuser and two measurements of the power were made, first without and then with the filter in the light path. The transmittance factor was computed as their ratio at each wavelength, at intervals of 0.5nm, and a 5-point median filter was applied to each curve to reduce noise (Fig. 5).

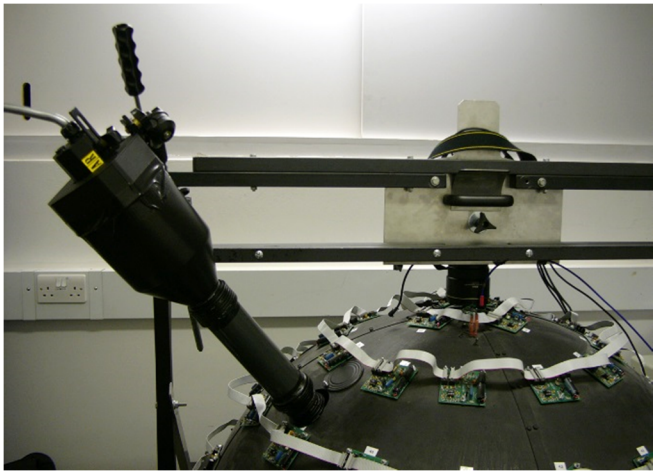

Figure 6. Setup with studio flash directed through narrow-band filter into dome.

The camera with zoom lens set to 55mm focal length and aperture f/2.8 was mounted in its usual position at the top of the UCL dome [11] and an X-rite ColorChecker White Balance target placed below on the baseboard. The illumination was generated by a Balcar xenon arc studio flash head inside a customised snoot with a transmission filter at the front. The light passed through a 25cm tube to collimate the beam, which was directed through one of the portholes at the side of the dome, at an elevation of 50° onto the white card below (Fig. 6). The fibre optic probe of the Ocean Optics HR2000+ spectrometer was fixed in position alongside the lens, pointing at the centre of the intensity distribution on the white card. A sequence of 16 images was captured, one for each filter, and the spectrum of the reflected illumination was simultaneously recorded by the spectrometer (Fig. 7).

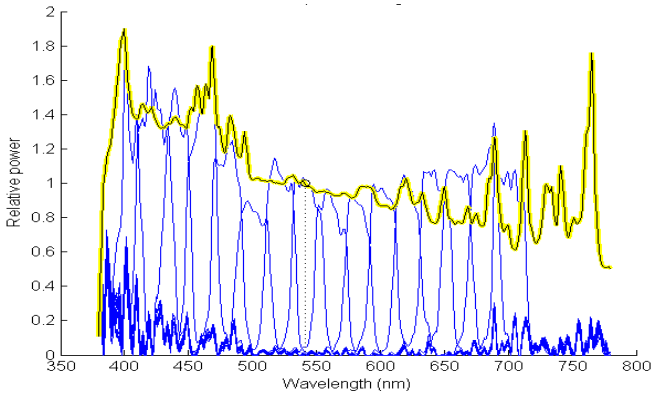

Figure 7. Measured spectral power distribution of Balcar flash illumination (yellow) and radiation transmitted through each filter (blue).

The camera responses were determined as the mean values in each of the R,G,B channels in a region of 200x200 pixels near the position of maximum intensity of the beam profile. Doing this for each of the 16 images corresponding to the 16 narrow-band transmission filters gave 16 points across the spectrum. After interpolation by cubic spline to 1nm intervals and correction for the integral power transmitted through each filter, the normalised sensitivity of the three channels could be compared with that measured by the monochromator (Fig. 8). The correspondence for green was excellent, but the widths of the curves for red and blue were slightly narrower by about 20nm in the upper half of their peak. At first it was thought that this may have been caused by the effects of measurement noise at either end of the spectrum, but it emerged that it was more likely due to the spiky illumination spectrum of the flash (see Section 7 below). The advantage of this method was that it was not necessary to know the spectrum of either the light source or the white card, because the spectrometer measured the same radiant spectrum entering the lens.

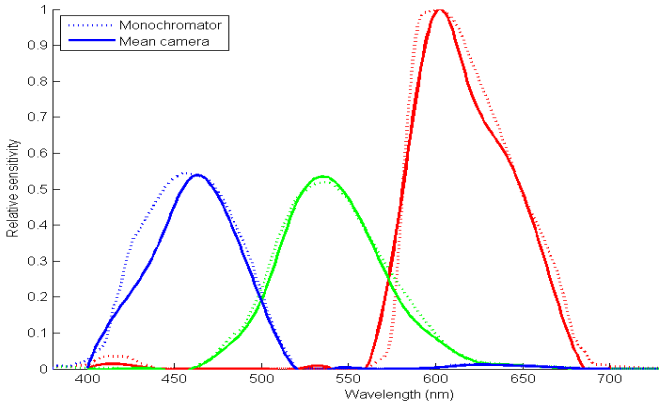

Figure 8. Corrected sensitivity of camera R,G,B for filtered flash illumination (solid lines) vs monochromator (dotted lines).

5. Multispectral Filters on Lens of Camera

The camera was mounted on a photographic copystand and a X-rite ColorChecker White Balance target placed on the baseboard. The same set of multispectral transmission filters was used as for the previous method, but this time the circular glass filters were screwed directly into the front of the lens housing. This ensured that no stray light entered the lens. The target was illuminated by a Bowens studio monobloc flash lamp with a large softbox diffuser (Fig. 9). This setup with an incident angle over a range of 20°–60° enabled the camera to capture the light reflected from the surface without specular highlights.

Figure 9. Camera with filter mounted on copystand with diffused flash lighting. Light reflected from white card was measured by PR-650 under PC control.

Images were processed in a similar way to the previous method, by cropping an area of 200x200 pixels out of the centre of each of the sixteen images and calculating the mean R,G,B values. Measurement of the reflected illumination from the white card was made by the PhotoResearch PR-650 spectroradiometer, mounted on a tripod. The advantage of measuring directly from the white card was that it was the same spectrum of reflected illumination as was entering the filter in front of the lens. Unlike the previous method described in Section 4, where the illumination was filtered and so changed for every exposure, in this case the illumination was constant (subject to the repeatability of the flash light) and so needed to be measured only once.

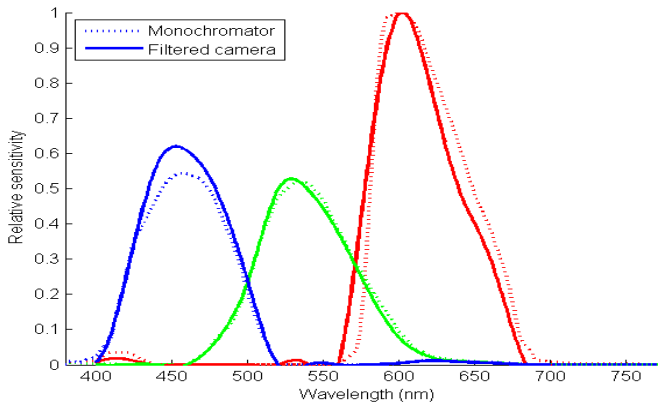

Figure 10. Corrected sensitivity of R,G,B for camera with multispectral filters and flash illumination (solid lines) vs monochromator (dotted lines).

After interpolation to 1nm intervals and correction for the integral power transmitted through each filter, the normalised sensitivity of the three channels (Fig. 10) could be compared with that measured by the monochromator. Although the green curves were near identical, differences were apparent in the other two curves: the base of red curve was shifted by ~10nm to shorter wavelengths, and the amplitude of the blue channel was greater.

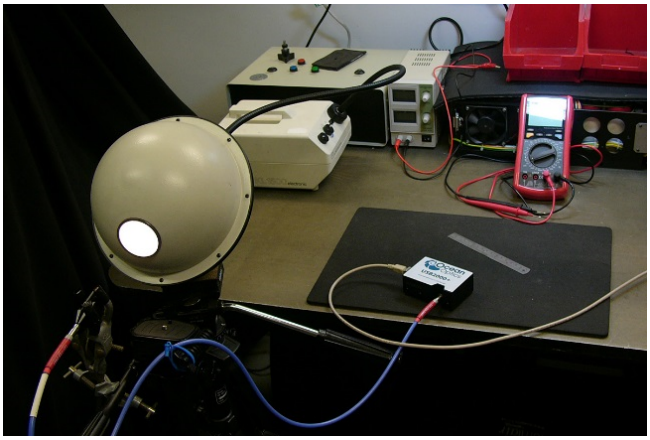

Figure 11. Setup for calibration measurement of USB2000+ spectrometer.

To explore the discrepancy further, the same procedure was repeated with a different source of lighting and a different spectroradiometer. The Kaiser fluorescent graphic arts lights were fitted on either side of the copystand, and an Ocean Optics USB2000+ spectrometer was coupled with an optical fibre, measuring the spectra at wavelength intervals of 0.35nm. Its radiance scale was corrected to that of the PR-650 by using the ratio of measurements by both instruments of light from a tungsten halogen lamp introduced into a 25 cm integrating sphere by an optical fibre bundle (Fig. 11). The resulting spectral power distribution of the fluorescent lights (Fig. 12) shows several very strong emission lines, with two in particular at 436 and 546 nm, characteristic of the mercury vapour discharge used within the tube to excite the phosphors. The results for the camera responsivity with the fluorescent illumination (Fig. 13), after the same procedure as before, showed a red curve similar to that for the filtered camera with flash illumination (Fig. 10), i.e. shifted by 10nm to the left.

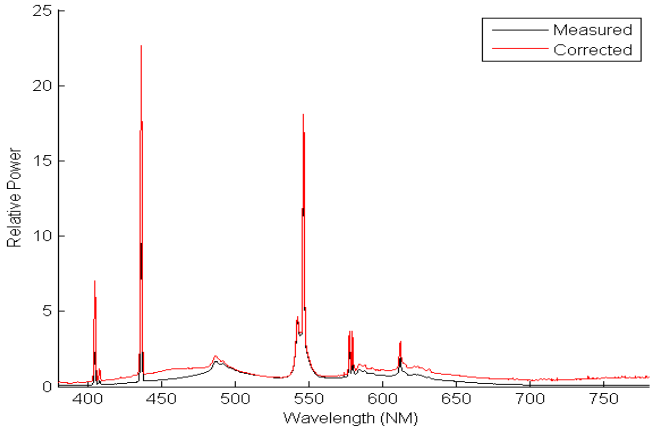

Figure 12. Measured and corrected spectral power distributions of Kaiser copystand fluorescent illumination reflected from white card.

However the green and blue curves were enlarged and distorted, and also the short-wave region of the red channel, which should have minimal response except for wavelengths in the range 400-430nm (violet).

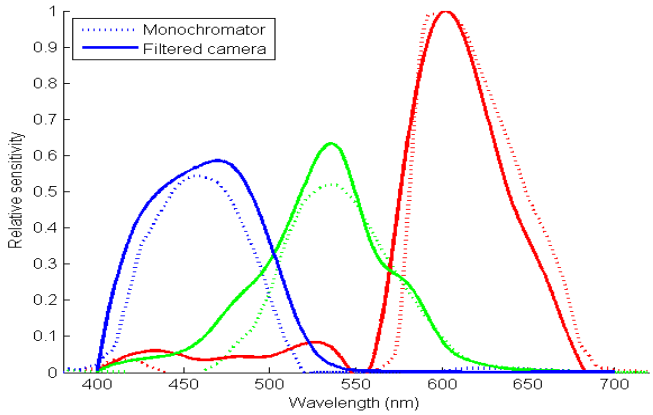

Figure 13. Corrected sensitivity of R,G,B for fluorescent illumination.

The procedure was repeated again on the copystand with Kaiser tungsten lights (a set of four 150W tungsten halogen bulbs). The results (Fig. 14) were much closer to the reference.

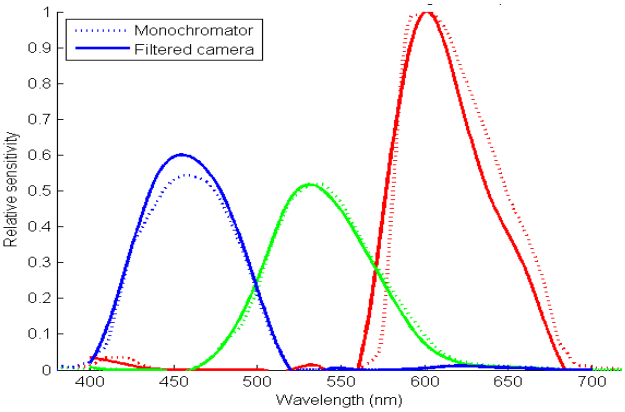

Figure 14. Corrected sensitivity of R,G,B for tungsten illumination.

6. Camera White Balance

The greater blue channel response found in all three cases when the filters were fitted on the camera lens (Figs. 10, 13 and 14) suggested that somehow the setting for colour balance (ratio of blue to red channels) in the camera may have been different in this case from when images were taken with the monochromator. The procedure was therefore repeated with six different settings of white balance in the Nikon software to determine the effect of this parameter. The settings were named in the Nikon menu as: Incandescent, Fluorescent, Sunlight, Flash, Cloudy, Shade.

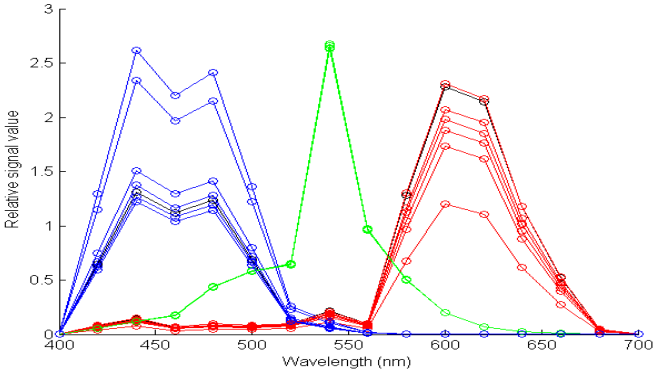

Figure 15. Mean RGB values for raw (black) and six settings of white balance.

It was found that if the raw images (NEF file format) were converted via DCRAW with the white balance option suppressed then all the resulting TIFF files were identical, apart from the effects of noise. If the white balance option was enabled in DCRAW, however, then the resulting TIFF files were different. Analysis by sampling a patch of 400x400 pixels from the centre of each image revealed further that the green channel never varied, but that the blue and red channels were each scaled by a constant factor relative to the corresponding raw values (Fig. 15). These were related inversely to the integrated power in the short and long wavelengths of the typical spectral power distribution for the given illumination (Table 1 and Fig. 16). Thus for incandescent illumination, for example, B was increased by a factor of 1.96, while R was reduced by a factor of 0.52, relative to G = 1.

Table 1. Nikon D200 – White balance correction ratios B:G:R

	Incand	Fluor	Sunlight	Flash	Cloudy	Shade
B	1.9687	1.7610	1.1575	0.9656	1.0372	0.9286
G	1.0000	1.0000	1.0000	1.0000	1.0000	1.0000
R	0.5201	0.7516	0.8212	0.9095	0.8679	1.0149

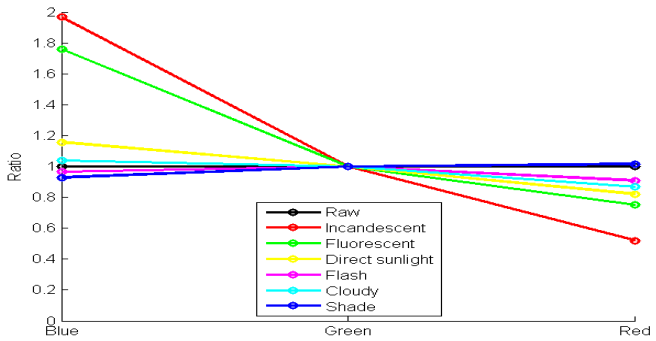

Figure 16. Ratios of blue and red channels relative to green for six settings of white balance.

The conclusion from this analysis is that the white balance setting does not affect the image data stored in the raw image file. It is just a parameter in the metadata associated with the image file. But, unless it is explicitly suppressed, the camera itself and all file conversion programs such as the Photoshop image processor, will apply these multiplicative factors to the image data, resulting in an apparent change of spectral responsivity. This is suggested as an explanation for the different relative amplitudes of the spectral sensitivity curves for the Nikon D200 published by Farrell *et al* [7].

7. Discussion

The white balance settings could not account for the shift in wavelength or changes in shape of the response curves in Figures 8, 10, 13 and 14. There must have been some other influence causing the observed change in responsivity. Either the spectral power measured by the spectrometer was too low or the signal response of the camera was too high in this region of the spectrum, causing the responsivity ratio of camera response to incident power to be too large. One explanation is that the spectroradiometric measurement of the spectral power distribution of the fluorescent light (Fig. 12) failed to capture the true amplitude and width of the spikes, resulting in a low estimate of luminous power. This might have been caused by saturation of the detector for the high amplitude of the spikes, or by the limited spectral resolution. The spectral dispersion of the grating is likely to be larger than the wavelength interval of the data delivered by the instrument. In either case the integral power of the illumination would be under-estimated.

Another explanation is that some sort of 'spectral leakage' was occurring through the filters. Because they are dichroic the transmittance spectra (Fig. 5) apply only for the normal angle of incidence and propagation of light through the body of the filter. Like all interference effects, the transmission changes with angle of incidence, shifting toward shorter wavelengths, approximated by:

$$\lambda(\theta) = \lambda_0 \sqrt{1 - \left(\frac{\sin\theta}{n}\right)^2} \qquad (1)$$

where: θ is the angle of incidence relative to the normal, λ_0 is the unshifted wavelength of the transmission at normal incidence, and n is the effective index of refraction inside the filter, which varies with polarisation [12]. In the arrangement of the camera mounted on the copystand, rays reflected from the white target can pass through the filter and thence through the lens in a cone of angles of up to 20° off the optical axis, depending on the lens aperture setting. The effect of Eq. (1) is shown in Fig. 17, assuming an index of refraction of 1.6 and normal wavelength of 580nm.

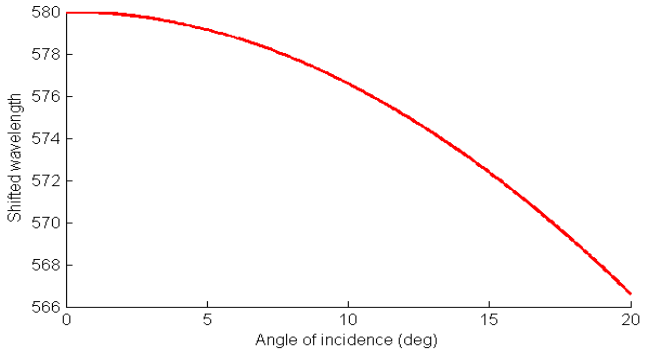

Figure 17. Shift in filter transmission wavelength with angle of incidence.

Thus, for example, the filter that normally transmits in the 20nm waveband 570–590nm would instead be transmitting in the band 556–576nm for an oblique ray of 20° incidence. The tail of the transmission spectrum would therefore be close to the emission spike at 546nm, resulting in a larger camera signal than expected, leading to the high values observed for both G and R responsivity curves at nominal 580nm (see Fig. 13). This effect could be minimised by masking the white card to a small area at centre of the image field and increasing the distance between camera and target.

8. Evaluation

In Figs. 4, 8, 10, 13 and 14 the spectral responsivities for the R,G,B camera channels determined by the respective methods were compared to that determined by the monochromator. All values were normalised and interpolated by cubic splines to 1nm intervals over the range 380-780nm. The differences were quantified in two ways: (1) difference in area between the curves; (2) rms difference of RGB camera signals. The first approach was to calculate:

$$d_k = \sum_\lambda \big(V_{n,k}(\lambda) - M_k(\lambda)\big)\, d\lambda \qquad (2)$$

where: d_k is the difference in area under curves for channel k = R,G,B; $V_{n,k}(\lambda)$ is responsivity of channel k for method n; $M_k(\lambda)$ is the responsivity of channel k for the monochromator; and $d\lambda$ is the wavelength interval = 1nm. The results are given in the first three columns of Table 2, showing that the differences for R were larger than for G and B, and that the method with the LED target gave the best results whereas a fluorescent source with filters on the camera gave the worst results.

The second approach started with a colorimetric calculation of the response of a camera with the given RGB responsivities:

$$s_k = \sum_\lambda L(\lambda)R(\lambda)V_{n,k}(\lambda)\, d\lambda \;/\; \sum_\lambda L(\lambda)V_{n,k}(\lambda)\, d\lambda \qquad (3)$$

where: s_k is the signal generated for channel k = R,G,B; $L(\lambda)$ is the power of the light source at wavelength λ; $R(\lambda)$ is the reflectance factor of the surface; and $V_{n,k}(\lambda)$ is the responsivity of channel k for method n. The calculation was then applied for the camera responsivities produced by each method for all 1950 samples in the NCS colour atlas under a D65 illuminant. Euclidean differences between these and the monochromator values were calculated as:

$$e_i = 255\sqrt{\Delta R_i{}^2 + \Delta G_i{}^2 + \Delta B_i{}^2} \qquad (4)$$

giving an error distribution of 1950 values in a linear 8-bit RGB space. The percentile values for 50% (median), 80% and 95% are given in the right three columns of Table 2, showing that the filtered flash illumination performed best, with the LED target second.

Table 2. Errors for five methods relative to monochromator

Method	R	G	B	50%	80%	95%
LED target	10.26	2.72	4.85	1.46	2.58	4.65
Filtered flash	10.77	2.95	6.35	1.04	2.12	3.82
Camera flash	14.81	3.32	5.21	1.84	3.86	6.73
Camera fluorescent	20.54	15.40	17.72	6.60	13.01	22.60
Camera tungsten	16.30	3.62	4.56	2.13	4.51	7.85

In conclusion, all the methods for characterising the camera's spectral responsivity gave consistent results, though all required careful setup. The one-shot LED target was very promising as an alternative to a monochromator. The set of 20nm multispectral filters gave usable results, and the method of illuminating a white card with filtered collimated light worked surprisingly well. The imaging geometry needs to be arranged so that the rays pass at angles near perpendicular to the filter plane. The large error values in all methods for the R channel, together with the consistent change in curve shape in the figures, suggests that the monochromator data may have been in error for R. For best performance a source with a smooth spectral power distribution such as tungsten or tungsten-halogen is recommended. In general, sources such as fluorescent with line emission spectra, producing high-amplitude spikes in the spectral power distribution, should be avoided because leakage of power from neighbouring bands can lead to loss of accuracy.

References

[1] P.L. Vora, J.E. Farrell, J.D. Tietz and D.H. Brainard. "Digital color cameras - 2 - Spectral response", Hewlett-Packard Technical Report, HP-97-54, 1997.

[2] F.M. Martínez-Verdú, J. Pujol and P. Capilla Perea, "Spectral responsivity vs action spectrum in digital photography", Proc. Intl. Conf. on Color in Graphics and Image Processing (CGIP), 2000.

[3] W. Wu and J.P. Allebach, "Imaging colorimetry using a digital camera", J. Imaging Science and Technology, 44(4) 267-279, 2000.

[4] L.W. MacDonald and W. Ji, "Colour characterisation of a high-resolution digital camera", Proc. Eur. Conf. on Colour in Graphics, Imaging and Vision (CGIV), Poitiers, France, 433-437, 2002.

[5] S.O. Park, H.S. Kim, J.M. Park and J.K. Eem. "Development of spectral sensitivity measurement system of image sensor devices", Proc. 3rd IS&T Color Imaging Conf., 115-118, 1995.

[6] P.M. Hubel, D. Sherman and J.E. Farrell, "A comparison of methods of sensor spectral sensitivity estimation", Proc. 2nd IS&T Color Imaging Conf., 45-48, 1994.

[7] J.E. Farrell, M. Okincha and M. Parmar, "Sensor calibration and simulation", Proc. SPIE Conf. on Digital Photography IV, SPIE Vol. 6817, 2008.

[8] D.S. Hawkins and P. Green, "Spectral characterisation of a digital still camera through a single integrating exposure", Proc. 4th IS&T Eur. Conf. on Colour in Graphics, Imaging and Vision (CGIV), 477-480, 2008.

[9] J.M. DiCarlo, G.E. Montgomery and S.W. Trovinger, "Emissive chart for imager calibration", Proc. 12th IS&T Color Imaging Conf., 295-301, 2004.

[10] L.W. MacDonald, A. Giacometti, A. Campagnolo, S. Robson, T. Weyrich, M. Terras and A. Gibson, "Multispectral imaging of degraded parchment", Computational Color Imaging, Springer, 143-157, 2013.

[11] L.W. MacDonald, A.H. Ahmadabadian and S. Robson, "Determining the coordinates of lamps in an illumination dome", Proc. SPIE Conf. on Videometrics and Range Imaging XIII, Vol. 9528, 2015.

[12] M.A. Quijada, C.T. Marx, R.G. Arendt and S.H. Moseley, "Angle-of-incidence effects in the spectral performance of the infrared array camera of the Spitzer Space Telescope", Astronomical Telescopes and Instrumentation, 244-252, 2004.

Author Biography

Lindsay MacDonald has divided his career between industrial R&D and academia. He received his PhD in image science from University College London (UCL) in 2015. He is a Fellow of IS&T and was General Co-Chair of the Color Imaging Conference in 1997. His research interests are in the application of imaging to cultural heritage, and anything related to colour.